



Aldol Condensation of Cyclopentanone with Valeraldehyde Over Metal Oxides

Päivi Mäki-Arvela¹ · Nataliya Shcherban^{1,2} · Chloé Lozachmeur¹ · Kari Eränen¹ · Atte Aho¹ · Annika Smeds¹ · Narendra Kumar¹ · Janne Peltonen³ · Markus Peurla⁴ · Vincenzo Russo⁵ · Konstantin P. Volcho^{6,7} · Dmitry Yu. Murzin¹

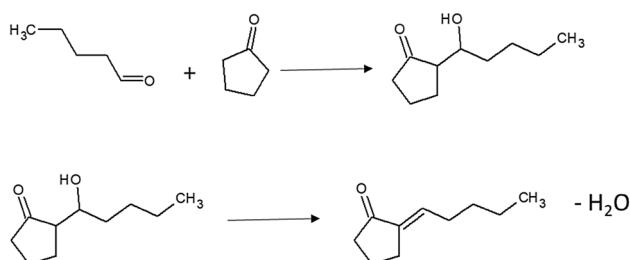
Received: 20 December 2018 / Accepted: 30 January 2019
© The Author(s) 2019

Abstract

Kinetics of the cross aldol condensation of valeraldehyde with cyclopentanone was investigated in a batch reactor under atmospheric pressure at 130 °C using heterogeneous metal modified oxides, such as CeO₂-MgO, FeO-MgO, FeO-CaO as well as pristine CaO as catalysts. The catalysts were prepared either by evaporation impregnation or deposition precipitation methods and characterized by XRD, TEM, SEM, nitrogen adsorption, ammonia and CO₂ TPD. The results revealed that an optimum amount of strong basic sites gives the highest ratio between cross condensation and self-condensation products of valeraldehyde. The highest yield of the desired product 2-pentylidenecyclopentanone (66%) was obtained with FeO-MgO prepared by the deposition precipitation methods.

Graphical Abstract

Cross-condensation of valeraldehyde with cyclopentanone was investigated over heterogeneous Fe-CaO, CeO-MgO, FeO-CaO and CaO catalysts at 130 °C using cyclopentanone as a solvent and reactant. The highest yield of the desired product, 2-pentylidene-cyclopentanone, finding applications as fragrances, flavours and pharmaceuticals, was 66% obtained over FeO-MgO catalyst exhibiting both acid and basic sites.



Keywords Basic catalyst · Aldol condensation · Valeraldehyde

Electronic supplementary material The online version of this article (<https://doi.org/10.1007/s10562-019-02701-1>) contains supplementary material, which is available to authorized users.

✉ Dmitry Yu. Murzin
dmurzin@abo.fi

¹ Johan Gadolin Process Chemistry Centre, Åbo Akademi University, Turku, Finland

² L.V. Pisarzhevsky Institute of Physical Chemistry, National Academy of Sciences of Ukraine, 31 pr. Nauky, Kiev 03028, Ukraine

³ Laboratory of Industrial Physics, University of Turku, Turku, Finland

⁴ Laboratory of Electron Microscopy, University of Turku, Turku, Finland

⁵ Università di Napoli Federico II, via Cintia, 4, 80126 Napoli, Italy

⁶ N. N. Vorozhtsov Institute of Organic Chemistry, Russian Academy of Sciences, Novosibirsk 630090, Russia

⁷ Novosibirsk State University, Novosibirsk 630090, Russia

List of symbols

K_j^0	Equilibrium constant at standard conditions for reaction j
n	Moles, mol
P	Pressure, bar
P^0	Standard pressure, bar
R	Ideal gas constant, J/K/mol
T	Absolute temperature, K
T^0	Absolute standard temperature, K

Greek symbols

ΔG_f^0	Gibbs free energy of formation at standard conditions, J/mol
ΔG_r^0	Gibbs free energy of reaction at standard conditions, J/mol
$\Delta G_{r,j}^\Phi$	Gibbs free energy of reaction at 1 bar and a chosen temperature, J/mol
ΔH_f^0	Enthalpy of formation at standard conditions, J/mol
ΔH_r^0	Enthalpy of reaction at standard conditions, J/mol
$\nu_{i,j}$	Stoichiometric matrix composed by i components and j reactions

1 Introduction

Several reactions are catalyzed by homogeneous and heterogeneous bases, including aldol condensation [1–4] and transesterification for product of biodiesel [5]. Aldol condensation is used for synthesis of various products ranging from

basic and specialty chemicals to fragrances, flavours and pharmaceuticals [1–5]. Conventionally aldol condensation is performed using homogeneous catalysts [6, 7], such as sodium or potassium hydroxide or $\text{Ti}(\text{O}-t\text{-Bu})_4$ as catalysts [7]. Aldol condensation of isophorone was recently demonstrated with furanic aldehydes using NaOH as a catalyst for production of jet fuels [4]. Heterogeneous catalysts could facilitate a more environmentally benign way to produce chemicals, as for example in alkaline earth metal-transition metal oxide in biodiesel production [5], or in aldol condensation due to their easy separation and reuse.

Very often heterogeneous base catalysts are also quite cheap, such as aluminophosphate [1] and hydrotalcites [2], active in synthesis of 2-pentylidencyclopentanone. In this work cross-condensation of valeraldehyde with cyclopentanone was investigated over several heterogeneous catalysts of basic nature, such as Ce–MgO, CaO and Fe-modified CaO and MgO. The aim was to study the influence of the type of base supports and methods of catalyst synthesis on the physico-chemical and catalytic properties in cross-condensation of valeraldehyde with cyclopentanone.

Besides cross-condensation per se several reactions (Fig. 1) can also occur, i.e. self-condensation of both valeraldehyde and cyclopentanone (Fig. S1) [4, 5]. In cross aldol condensation the first step is formation of hydroxylated 1-hydroxy-2-pentylcyclopentanone **3**, which in the consecutive step undergoes dehydration forming an unsaturated ketone, 2-pentylidencyclopentanone **4**. This ketone being the desired product, can further react with another aldehyde forming 2,5-dipentylidencyclopentanone **7**.

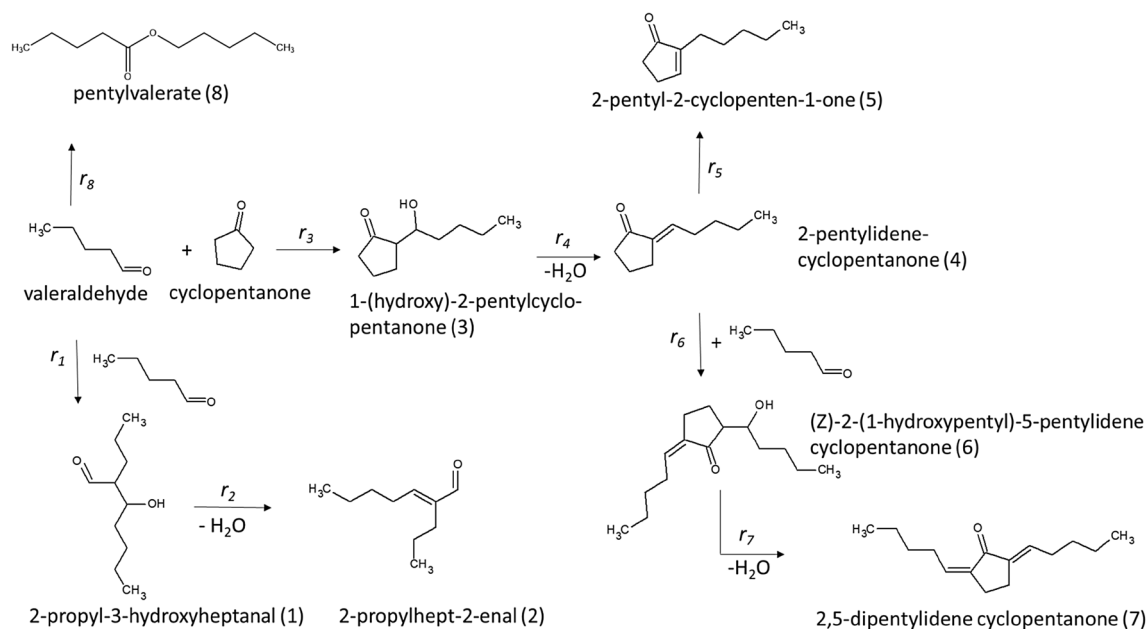


Fig. 1 Reaction scheme for valeraldehyde condensation with cyclopentanone

Cross-aldol condensation of valeraldehyde with cyclopentanone has been very scarcely studied over heterogeneous catalysts [1, 2]. The desired product **4**, 2-pentylidene-cyclopentanone has been synthesized over heterogeneous hydrothermalites as catalysts giving maximally 90% yield using valeraldehyde to cyclopentanone molar ratio of 1:5 at 80 °C after 11 h via slowly adding valeraldehyde into the reactor containing cyclopentanone [2]. In another work also an excess of cyclopentanone was used in comparison with valeraldehyde in *m*-xylene as a solvent at 130 °C under nitrogen [1]. The highest selectivity of 2-pentylidene-cyclopentanone, 91% at 31% conversion, was obtained at 130 °C after 2 h using amorphous aluminosilicate as a catalyst.

Other reactions relevant to aldol condensation, namely self-condensation of cyclopentanone and valeraldehyde, have been also investigated. Self-condensation of cyclopentanone gives 2-cyclopentylidene-cyclopentanone, which finds applications as fuel or in hydrogenated form as fragrances and flavors [8, 9]. This reaction occurs using potassium hydroxide as a catalyst, for example at 100 °C [8], followed by extraction with diethylether, washing and drying finally giving 73% yield. More recently also heterogeneous catalysts have been used in the synthesis of 2-cyclopentylidene-cyclopentanone by self-condensation of cyclopentanone [10]. Mesoporous MgO–ZrO₂ gave two main products, namely 2-cyclopentylidene-cyclopentanone composed of 10 carbon atoms and 2,5-dicyclopentylidene-cyclopentanone [10]. A remarkable excess of the former product with 100% selectivity was obtained after 4.5 h at 8% conversion using a lower reaction temperature 110 °C. On the contrary at 130 °C selectivity was 92% at 85% conversion. The same reaction was also investigated with MOF encapsulated phosphotungstic acid as a catalyst at 130 °C under nitrogen [11]. The yield of 2-cyclopentylidene-cyclopentanone was only ca. 12% after 2 h because of its further transformation to trimeric compounds and after removal of hydrogen to trindane.

Self-condensation of valeraldehyde gives 2-propylhept-2-enal, which has found applications as an intermediate for production of perfumes [12], and plasticizers [13, 14]. Aqueous NaOH is typically applied as a catalyst in industrial scale for this reaction. It was pointed out [13], that this process causes corrosion and exhibits poor product selectivity. TiO₂ was confirmed to be an efficient heterogeneous catalyst for synthesis of 2-propylhept-2-enal giving very high selectivities to the desired product at 190 °C [13]. Zhao et al. [13] stated that acidity is also required for production of 2-propylhept-2-enal.

In the current work metal oxides have been applied as catalysts in aldol condensation of valeraldehyde with cyclopentanone. Since it is known that aldol condensation requires acids or bases as catalysts [15], basic supports such as CaO and MgO were modified with ceria and iron oxide,

because of amphoteric nature of ceria and Lewis acidity of iron oxide. Therefore, not surprisingly, iron oxides have been used as catalysts in cyclohexanone aldol condensation [16], while cesium was utilized in aldol condensation of heptanal with benzaldehyde [17]. The aim in this work was to reveal the role of basic and acid active sites, metal functions in aldol condensation of valeraldehyde with cyclopentanone and investigate reaction kinetics and thermodynamics. The acidity and basicity of the catalysts were quantified by NH₃ and CO₂ temperature programmed desorption techniques. According to our knowledge this is the first time when kinetics and thermodynamics of valeraldehyde–cyclopentanone aldol condensation are reported.

2 Experimental Section

2.1 Catalyst Synthesis

Fe-modified MgO and CaO and Ce-modified MgO catalysts were prepared using deposition precipitation (DP) and evaporation impregnation (EIM) methods. The CeO₂–MgO–DP catalyst was prepared via dissolving cerium nitrate in distilled water adding thereafter MgO into the cerium nitrate aqueous solution. In the deposition–precipitation procedure, pH was first increased to 10 with ammonium hydroxide solution (25%) to precipitate cerium followed by stirring the slurry at 150 rpm for 24 h. After that, the catalyst was filtered and washed with distilled water. CeO₂–MgO–DP catalyst was dried in an oven at 100 °C for 7 h. Decomposition of cerium nitrate was carried out by thermal treatment of CeO₂–MgO–DP catalyst in a muffle oven using a step calcination procedure. The catalyst designated as CeO₂–MgO–DP.

FeO–MgO–DP catalyst was prepared using aqueous solution of ferric nitrate by a deposition precipitation method. The pH was increased to 10 using ammonium hydroxide solution (25%) and the synthesis carried out for 24 h, which was followed by drying at 100 °C for 7 h and calcination in a muffle oven. The catalyst designated as Fe–MgO–DP.

The aqueous solution of the ferric nitrate precursor was mixed with CaO and kept in a rotary evaporator for 24 h at the stirring speed of 50 rpm. In the subsequent step, the water phase was evaporated. The catalyst was removed from the rotatory flask and dried in an oven at 100 °C for 7 h. Decomposition of cerium nitrate was carried out in a muffle oven at 450 °C for 4 h using a step calcination procedure. The catalyst was designated as Fe–CaO–EIM.

2.2 Catalyst Characterization Methods

The Philips X'Pert Pro MPD X-ray powder diffractometer was used in the XRD measurements. The diffractometer

was operated in Bragg–Brentano diffraction mode, and the monochromatized Cu–K α radiation ($\lambda = 1.541874 \text{ \AA}$) was generated with a voltage of 40 kV and a current of 45 mA. The measured diffractograms were analyzed with Philips X'Pert HighScore and MAUD [18] programs. The Powder Diffraction File 2 (PDF-2) database, Inorganic Crystal Structure Database (ICSD), and Crystallography Open Database (COD) were used as references [19–21].

The scanning electron microscopy coupled with an energy dispersive X-ray analyzer was utilized to study morphology of the fresh catalysts using Zeiss Leo Gemini 1530 microscope combined with secondary electron and back-scattered electron detectors. Acceleration voltage of 15 kV was used for X-ray analyzer. In order to perform analysis, the catalyst was placed as a thin layer on top of the carbon coating to enhance the conductivity and allow high quality of magnified images.

The transmission electron microscopy was utilized to study the structural properties, porosity, metal particle size and distribution using JEM-1400Plus (by JEOL Ltd. Japan) of 120 kV maximal acceleration voltage. Interpretation of TEM images and determination of the particles sizes of the fresh and spent catalyst were done using ImageJ program.

The specific surface area was determined with Sorptometer 1900 (Carlo Erba Instrument) using nitrogen physisorption. The catalysts were outgassed at 150 °C for 3 h prior to the measurement. The BET equation was used to calculate the specific surface area.

CO₂ TPD measurements were performed to determine the concentration of basic sites using Autochem 2010, Micromeritics instrument. The catalyst, 200 mg, was first dried at 150 °C for 30 min under helium (AGA, 99.996%) after which it was cooled to 100 °C. Thereafter CO₂ (AGA) was adsorbed on the catalyst surface during 30 min. The physisorbed CO₂ was flushed from the catalyst surface at 100 °C for 30 min after which the temperature was increased by 10 °C/min up to 700 °C.

Ammonia TPD was performed with Micromeritics (AutoChem 2910) using helium as a carrier gas. The sample was dried prior to the measurement at 250 °C for 30 min after which ammonia (5 vol% in helium, AGA) was adsorbed on the catalyst for 60 min at 25 °C. Then the gas supply was stopped and these conditions were hold for 30 min. In the next step the temperature was increased by 10 °C/min to 100 °C and hold at 100 °C for 30 min. The ammonia TPD was measured using the following temperature programme: 100 °C–10 °C/min–600 °C.

2.3 Kinetic Experiments

Catalytic experiments were typically performed under flowing helium at 130 °C in a glass reactor equipped with a stirrer. Typically valeraldehyde (Aldrich, 97%) was reacting

with an excess of cyclopentanone (Sigma Aldrich, > 99%), which was also applied as a solvent (60 ml), if not otherwise stated. The initial valeraldehyde concentration was 0.50 mol/l if not specifically mentioned. The experiments were performed by adding valeraldehyde, cyclopentanone and the catalyst into the cold reactor, which was then heated to 130 °C. The reactor system was equipped with a condenser, which exhibited temperature close to zero. Valeraldehyde and a part of cyclohexanone were thus condensed back to the liquid phase. The experiments were carried out under argon atmosphere. The weight ratio of valeraldehyde to cyclopentanone in the kinetic experiments was 0.05, while the amount of catalyst was 1.6 g. The mass ratio of valeraldehyde to catalyst was 1.7 being the same as was used in [1]. Small catalyst particles (below 63 μm) were used under vigorous stirring (600 rpm) to avoid internal and external mass transfer limitations. In some experiments mesitylene (Sigma Aldrich, 97%) was used as a solvent. The products were analyzed by a GC equipped with HP-5 column (30 m, $d_i=320 \mu\text{m}$, film thickness 0.5 μm) using the following temperature programme: 60 °C (2 min)–8 °C/min–124 °C–4 °C/min–200 °C–12 °C/min–280 °C (10 min). The reaction products were identified by GC–MS (Agilent Technologies, 6870N) equipped with DB-1 column (30 m, 250 μm , film thickness 0.50 μm).

3 Results and Discussion

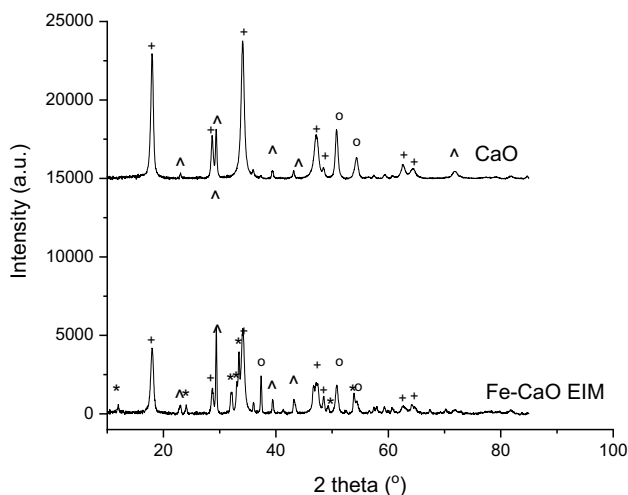
3.1 Catalyst Characterization Results

XRD results revealed that FeO–CaO–EIM catalyst contained iron only as Ca₂Fe₂O₅ phase (Table 1; Fig. 2). Ca₂Fe₂O₅ in [22] was prepared by coprecipitation of Ca and Fe nitrates and calcined at 500 °C. The size of Ca₂Fe₂O₅ is about 60 nm based on XRD [23]. On the other hand, metal oxide Fe₂O₃ particles are threefold smaller than Ca₂Fe₂O₅ (Table 1). XRD results of CeO₂–MgO showed the presence of cubic CeO₂ [24] and MgO [28] (Table 2). XRD of FeO–MgO–DP displayed only the presence of cubic MgO. This result indicates that iron either is in an amorphous form or it well dispersed on the support with the particle size below 3 nm, not being detectable by XRD.

SEM images of different catalysts are depicted in Fig. 3. CeO₂–DP exhibits both spherical and plate-like character (Fig. 3a). FeO–MgO–DP contains plates (Fig. 3b) whereas FeO–CaO–EIM exhibited large spherical particles between 105 and 148 nm (Fig. 3c). Particles in FeO–CaO–EIM were both of irregular and spherical shapes in the range of 50 to 600 nm (Fig. 3d). The particle sizes in CaO varied in a broader range of 50 to 400 nm. These changes can be related to the presence of different phases in these materials. CaO is

Table 1 Phase composition and particle size of CaO and FeO–CaO–EIM determined by XRD [24, 25]

Phase	Framework	hkl at 2 θ (°)	CaO		FeO–CaO–EIM	
			wt%	D (nm)	wt%	D (nm)
CaCO ₃	Rhombohedral	104 (29.40), 018 (47.38)	16 ± 6	38 ± 25	19 ± 17	92 ± 55
Ca(OH) ₂	Hexagonal	001 (17.98), 104 (29.40), 101(34.12), 102 (47.38)	83 ± 5	26 ± 6	52 ± 6	24 ± 7
Fe ₂ O ₃	Rhombohedral	104 (33.18), 024 (49.52)	0	0	0	0
Ca ₂ Fe ₂ O ₅	Orthorhombic	020 (11.99), 002, (32.00), 200 (33.06), 141 (33.49)	0	0	22 ± 8	60 ± 12
CaO	Cubic	200 (37.38), 220 (53.90)	1 ± 1	n.d	7 ± 3	65 ± 30

**Fig. 2** XRD patterns from CaO, and FeO–CaO–EIM. Notation: Ca(OH)₂+, CaCO₃^, CaO o, Ca₂Fe₂O₅*, Fe₂O₃#**Table 2** Phase composition and particle size of FeO–MgO–DP and CeO₂–MgO catalysts determined by XRD [24, 26–28]

Catalyst	Phase	Framework	wt%	D (nm)
FeO–MgO–DP	MgO	Cubic	100	20 ± 2.0
CeO ₂ –MgO–DP	CeO ₂	Cubic	31 ± 19	9.0 ± 2.0
	MgO	Cubic	69 ± 19	17 ± 3

rich in hexagonal Ca(OH)₂, however, FeO–CaO–EIM contained mainly CaCO₃.

The TEM images showed also large differences in the particle sizes and shapes (Fig. 4). FeO–CaO–EIM contains spherical particles (Fig. 4a), whereas the parent CaO exhibited 10 to 50 nm particles which were not easy to separate from each other.

Basicity determined by CO₂ temperature programmed desorption showed that pure CaO exhibited the highest basicity in accordance with the literature (Table 3; Fig. 5a) [23, 29]. CaO contained large amounts of medium and strong acid sites. When CaO was modified by Fe using the evaporation impregnation method its basicity decreased to

59% of the initial value for pristine CaO due to a relatively high Fe loading, 10%. In addition the concentration of strong basic sites decreased in this catalyst by iron modification being only 21% of that of CaO. Nevertheless, basicity of FeO–CaO–EIM was quite high, partially due to high basicity of Ca₂Fe₂O₅ (Fig. 5a) [5], which was comparative to the parent CaO. The composite material CeO₂–MgO–DP with 24 wt% Ce exhibited a total basicity higher than the pristine MgO. The amount of strong basic sites in both CeO₂–MgO–DP was, however, quite low compared to the parent MgO, which according to the literature exhibits more strong basic sites than CeO₂ [30].

Acidity, determined by ammonia TPD, follows the order (Table 3; Fig. 5 b): 21 wt% CeO₂–MgO–DP > 10 wt% FeO–CaO–EIM > 7 wt% FeO–MgO–DP. The lowest acidity was measured for FeO–MgO–DP, containing the lowest metal amount. In fact for this material no Fe₂O₃ was observed according to XRD (Table 2) and most probable iron is present in the form of finely dispersed iron oxide particles. Results in Table 3 showing some acidity for FeO–MgO–DP can be interpreted by taking into account that Fe₂O₃ exhibits both Brønsted and Lewis acidity [31]. The highest acidity of CeO₂–MgO–DP is explained by its high CeO₂ loading. It is known that CeO₂ is amphoteric which influences its acidic and basic properties. Acidity of 10 wt% FeO–CaO–EIM is related to presence of iron + 3 possessing Lewis acidity [32] in the form of Ca₂Fe₂O₅.

3.2 Reaction Network and Thermodynamic Analysis

The reaction network for aldol condensation of valeraldehyde with cyclopentanone is shown in Fig. 1. It should be pointed out here, that as mentioned in the Introduction self-condensation of cyclopentanone forming 2-cyclopentylidene-cyclopentanone, requires presence of strong basicity, thus its contribution to valeraldehyde self- and cross-condensation reactions was considered to be less significant. According to the literature [2] valeraldehyde condensation proceeds via formation of an intermediate 1-hydroxy-2-pentylcyclopentanone **3**, which is dehydrated forming the desired product 2-pentylidenecyclopentanone **4**. In addition

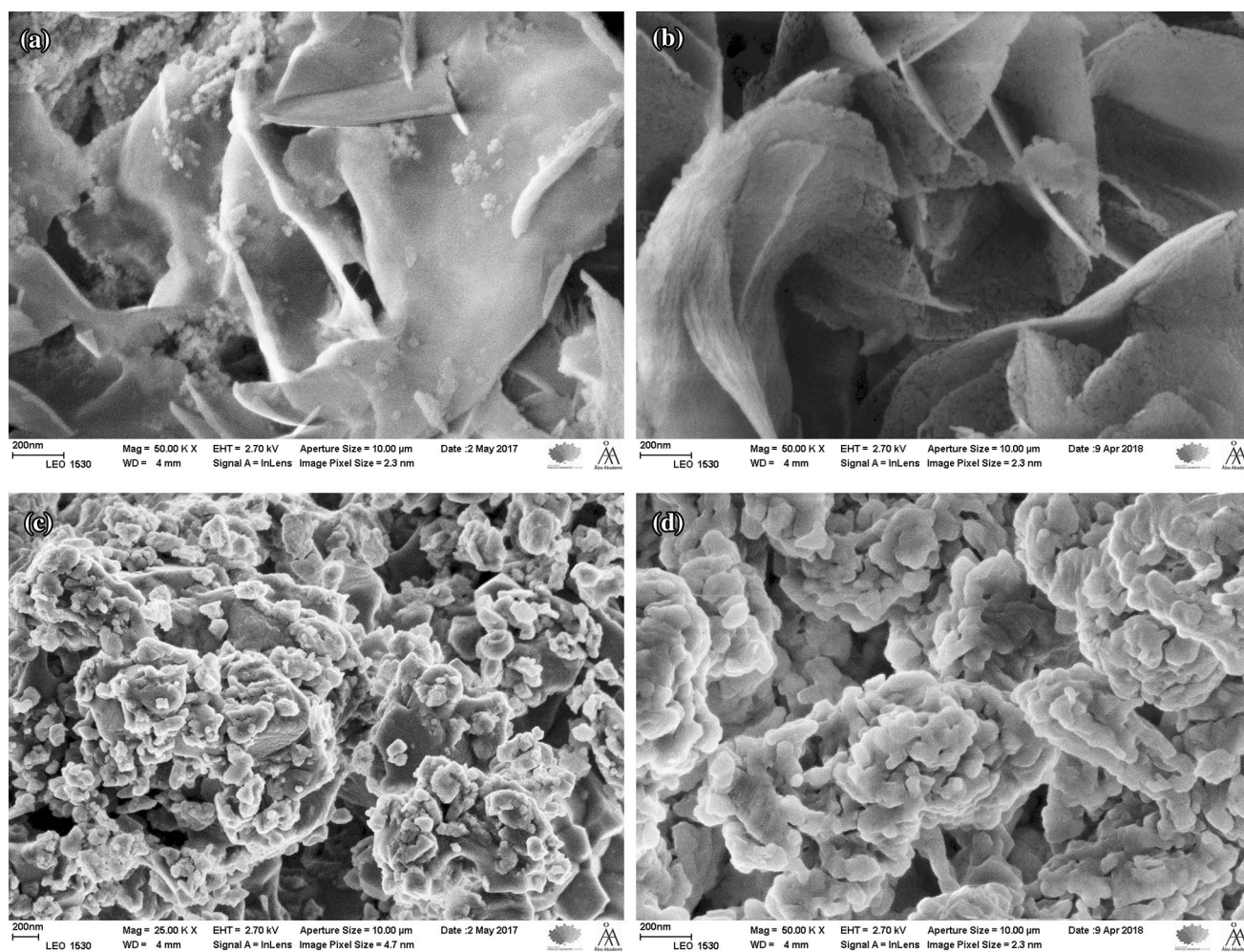
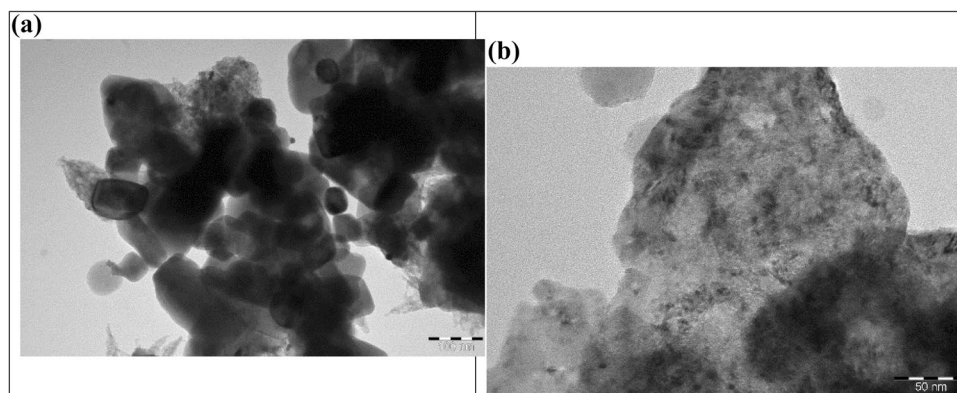


Fig. 3 SEM images of **a** CeO₂-MgO-DP, **b** FeO-MgO-DP, **c** FeO-CaO-EIM, and **d** CaO

Fig. 4 TEM images of **a** FeO-CaO-EIM, **b** CaO

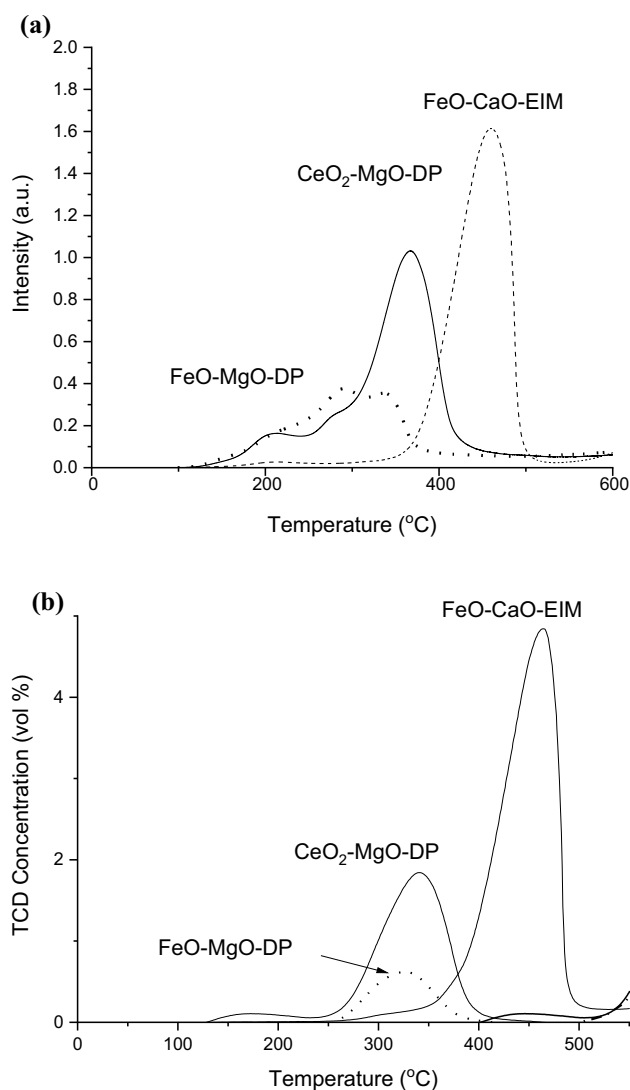


to formation of the desired cross-condensation product, the latter can also be isomerized to 2-pentyl-2-cyclopenten-1-one **5**, especially at higher temperature, when this isomer is thermodynamically more stable than the desired product **4** [2]. The desired product can also react further with another

valeraldehyde molecule giving 2-(1-hydropentyl)-5-pentylidene cyclopentanone **6** and its corresponding dehydrated product, 2,5-dipentylidene cyclopentanone **7**. Furthermore, other reactions can also occur, namely self-condensation of valeraldehyde giving 2-propyl-3-hydroxyheptanal, **1** which

Table 3 Metal content, basicity and acidity of the catalysts

Catalyst	Metal content by EDXA (wt%)	Amount of basic sites				Amount of NH ₃ desorbed (μmol/g _{cat})	T _{max} (°C) for ammonia desorption
		Weak (desorbed below 277°C) μmol/g _{cat}	Medium (desorbed between 277–477 °C) μmol/g _{cat}	Strong (desorbed above 477 °C) μmol/g _{cat}	Sum of basic sites		
CaO	0	22	905	1179	2105	n.d	n.d
FeO–CaO–EIM	10	13	962	259	1234	305	430
MgO	0	99	731	168	989	n.d	n.d
FeO–MgO–DP	7.0	222	354	118	695	45	306
CeO ₂ –MgO DP	24	76	967	43	1087	152	380

**Fig. 5** a CO₂ TPD of FeO–CaO–EIM, FeO–MgO–DP and CeO₂–MgO–DP, b NH₃ TPD of FeO–CaO–EIM and CeO₂–MgO–DP

can be dehydrated to the corresponding unsaturated aldehyde, 2-propylhept-2-enal **2**. In the current case no pentyl

valerate **8** could be seen, which in general can be formed via the Tischenko reaction.

Aldol condensation can occur both on basic and acid sites according to the literature suggestions [2]. Cross aldol condensation over basic sites can be described by a mechanism, [2] when the base accepts a proton from the ketone forming in the current case negatively charged O[−] in cyclopentanone which attacks the aldehyde via a nucleophile forming hydroxypentylcyclopentanone. Dehydration occurs via formation of a carbocation which after deprotonation gives 2-pentylidenecyclopentanone.

In acid catalyzed aldol condensation the reaction has been proposed to start with enolization of the aldehyde over Lewis acid sites. Subsequently the carbocation formed from the aldehyde on Brønsted acid site reacts with the enol leading to formation of a cross condensation product [33].

While the main focus in this work was on kinetics of the cross condensation of valeraldehyde with cyclopentanone, in order to understand if thermodynamics governs the overall reaction, first thermodynamic analysis was performed. According to our knowledge thermodynamics for the cross condensation and relevant reactions has not been reported. Evaluation of thermodynamics was done by calculating enthalpy (ΔH_r^0) and Gibbs free energy (ΔG_r^0) at standard conditions using the approach from [34] and starting from the standard enthalpy (ΔH_f^0) and Gibbs free energy (ΔG_f^0) of formation from the elements estimated with the Joback approach [35–37]:

$$\Delta H_{r,j}^0 = \sum_j v_{i,j} \cdot \Delta H_{f,i}^0 \quad (1)$$

$$\Delta G_{r,j}^0 = \sum_j v_{i,j} \cdot \Delta G_{f,i}^0 \quad (2)$$

The equilibrium constant of each reaction was calculated from its definition

$$K_j^0 = \exp\left(-\frac{\Delta G_{r,i}^0}{RT}\right) \quad (3)$$

Table 4 Enthalpy and Gibbs free energy formation for each component (*i*) (given in bold) and stoichiometric matrix for component *i* for reaction *j*

Component	ΔH_f^0 (kJ/mol)	ΔG_f^0 (kJ/mol)	<i>i/j</i>	1	2	3	4	5	6	7	8
Valeraldehyde	-232	-108	1	-2	0	-1	0	0	-1	0	-2
2-Propyl-3-hydroxyheptanal	-498	-20.8	2	1	-1	0	0	0	0	0	0
2-Propylhept-2-enal	-228	5.47	3	0	1	0	0	0	0	0	0
Cyclopentanone	-195	-87.1	4	0	0	-1	0	0	0	0	0
1-Hydroxy-2-pentylcyclopentanone	-484	-192	5	0	0	1	-1	0	0	0	0
Water	-242	-228	6	0	1	0	1	0	0	1	0
2-Pentylidenecyclopentanone	-231	0.45	7	0	0	0	1	-1	-1	0	0
2-Pentyl-2-cyclopenten-1-one	-260	-24.7	8	0	0	0	0	1	0	0	0
(<i>Z</i>)-2-(1-hydroxypentyl)-5-2-pentylidenecyclopentanone	-512	-104	9	0	0	0	0	0	1	-1	0
2,5-Dipentylidene cyclopentanone	-258	88.0	10	0	0	0	0	0	0	1	0
Pentyl-valerate	-495	-201	11	0	0	0	0	0	0	0	1

Table 5 Enthalpy and Gibbs free energy for each reaction (*j*) at standard conditions, equilibrium constants at standard conditions (K_j^0)

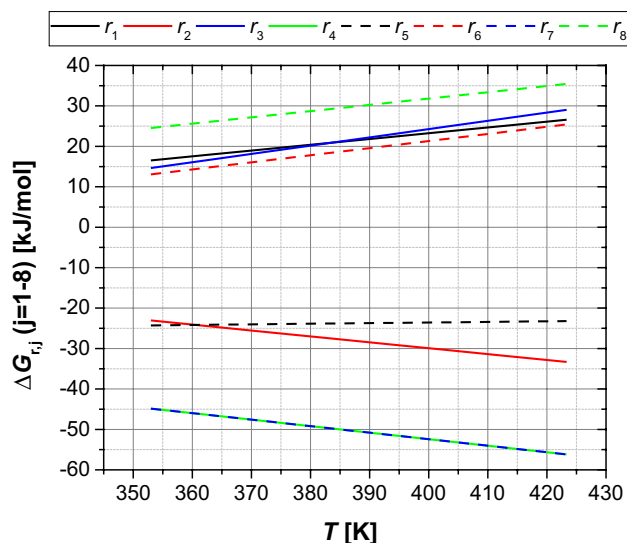
<i>j</i>	ΔH_{rj}^0 (kJ/mol)	ΔG_{rj}^0 (kJ/mol)	K_j^0
1	-33.9	0.87	2.99×10^{-2}
2	28.4	-15.1	4.37×10^2
3	-57.6	0.34	2.51×10^{-1}
4	12.1	-36.0	2.04×10^6
5	-29.7	-25.1	2.53×10^4
6	-48.9	0.34	2.51×10^{-1}
7	12.1	-36.0	2.04×10^6
8	-30.3	16.0	1.57×10^{-3}

The dependence of the reaction free Gibbs energy on temperature was included by implementing the Gibbs–Helmholtz equation valid at $P=1$ bar (ΔG_{rj}^ϕ)

$$\frac{\Delta G_{rj}^\phi(T)}{T} = \frac{\Delta G_{rj}^0}{T^0} + \Delta H_{rj}^0 \left(\frac{1}{T} - \frac{1}{T^0} \right) \quad (4)$$

The calculated enthalpy and Gibbs free energy formation for each component (*i*) are reported in Table 4. Numbering of reactions is from Fig. 1.

Starting from these values, the enthalpy and Gibbs free energy for each reaction (*j*) at standard conditions, equilibrium constants at standard conditions (K_j^0), enthalpy and Gibbs free energy at different temperatures and pressure were calculated. A temperature range between $T_{min}=353.15$ K and $T_{max}=423.15$ K was investigated. It can be seen that thermodynamically most favorable reactions are 4 and 7, namely dehydration of the intermediate

**Fig. 6** Gibbs free energy for each reaction (*j*) as a function of temperature

2-hydroxyl-2-pentylcyclopentanone to the desired product and formation of 2,5-dipentylidene cyclopentanone (Table 5; Fig. 6). It can also be seen from Fig. 6 that both of these reactions become even more thermodynamically feasible at higher temperatures. Interestingly the ΔG for formation of 2-pentyl-2-cyclopentyl-1-one, isomer of the desired product, was independent on temperature.

3.3 Catalytic Results

In the preliminary work valeraldehyde condensation with cyclopentanone was investigated using mesitylene as a solvent, since in [1] successful aldol condensation in this reaction was reported to occur in another substituted aromatic compound, *o*-xylene, as a solvent. In the current work

aldol condensation of valeraldehyde with cyclopentanone was performed analogously to the work of Hasni et al. [1] using 1:5 molar ratio of the reactants, however, instead of *m*-xylene in mesitylene as a solvent over CeO₂-MgO-DP. The results showed, however, that with a low initial valeraldehyde concentration (0.09 mol/l) in mesitylene as a solvent, mainly self-condensation products of valeraldehyde (98%) were formed in 3 h at 56% conversion at 130 °C, when 1:5 molar ratio of valeraldehyde to cyclopentanone was applied. In addition, minor oxidation of mesitylene occurred resulting in formation of 3,5-dimethylbenzaldehyde, confirmed by GC-MS, which might be possible by lattice oxygen originating from CeO₂. After the initial experiments in mesitylene as a solvent, valeraldehyde condensation was subsequently performed using cyclopentanone both as a solvent and a reactant.

Both the thermal reaction between valeraldehyde and cyclohexanone in the absence of any catalyst as well as catalytic experiments were carried out using an excess of cyclopentanone. The concentration profiles for valeraldehyde and its self- and cross-condensation products are shown in Figs. 7, 8, 9, 10, 11, 12. In thermal cross condensation of valeraldehyde at the initial concentration of 0.53 mol/l 95% conversion of valeraldehyde was obtained. The main product was 2-propylhept-2-enal. In addition relative large amounts of both 2-propyl-3-hydroxyheptanal, identified based on the confirmation of the *m/z* + peak at 173 in GC-MS analysis reported in [38] and 1-hydroxy-2-pentylcyclopentanone and

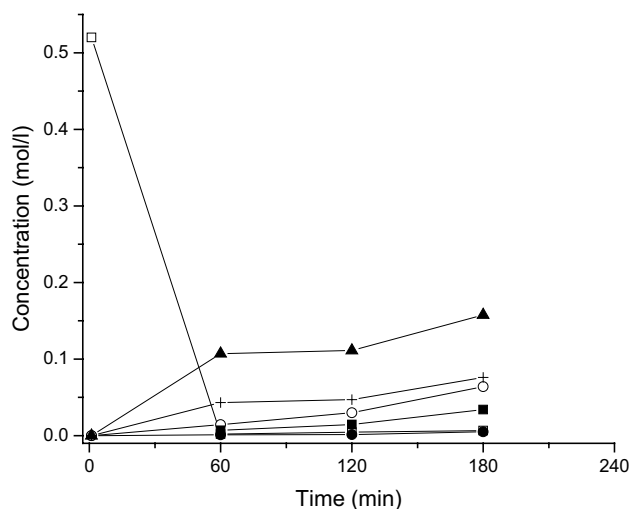


Fig. 7 Concentration of valeraldehyde and its self- and cross-condensation products as a function of time in valeraldehyde cross-condensation with cyclopentanone. The initial valeraldehyde concentration was 0.53 mol/l in cyclohexane. The experiments were performed at 130 °C under argon flow. Symbols: valeraldehyde (white square), 2-pentylidenecyclopentanone **4** (black circle), 2-pentyl-2-cyclopent-1-one **5** (white circle), 2-propyl-3-hydroxyheptanal (+) **1**, 2-propylhept-2-enal (black up-pointing triangle) **2** and 1-hydroxy-2-pentylcyclopentanone (black square) **3**

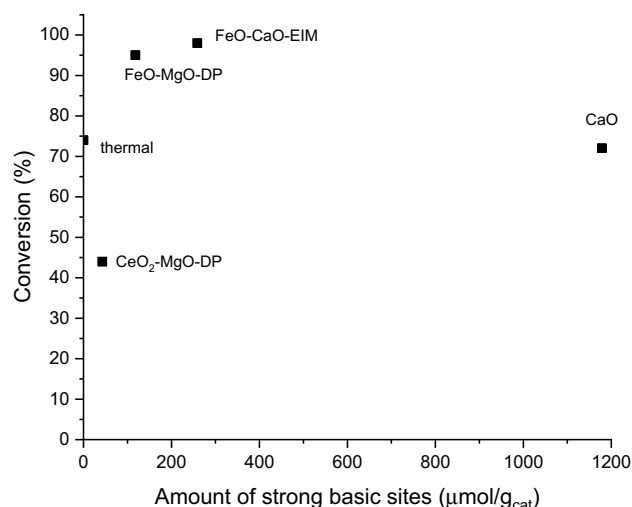


Fig. 8 Conversion of valeraldehyde after 1 h. The initial valeraldehyde concentration was 0.53 mol/l in cyclohexane. The experiments were performed at 130 °C under argon flow

an isomer of the desired 2-pentyl-2-cyclopent-1-one were formed. This result clearly shows that valeraldehyde self-condensation does not require any catalyst under the studied conditions. In addition the isomerization of the desired product, 2-pentylidenecyclopentanone can occur, especially at relatively high temperatures due to the fact that 2-cyclopent-1-one **5** is thermodynamically more stable than **4** due

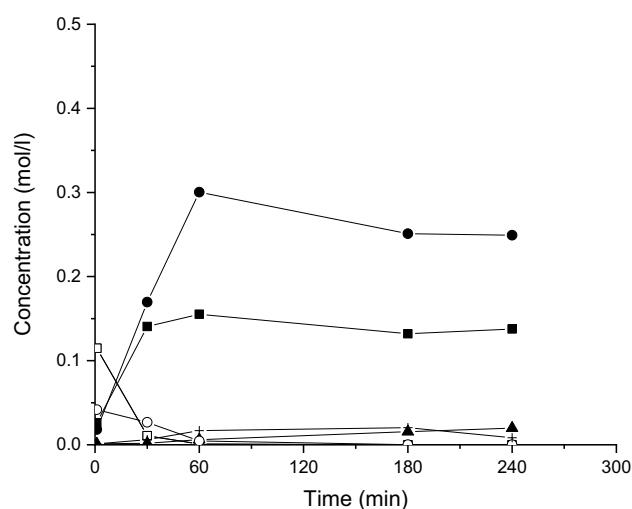


Fig. 9 Concentration of valeraldehyde and its self- and cross-condensation products as a function of time in valeraldehyde cross-condensation with cyclopentanone over FeO-CaO-EIM. The initial valeraldehyde concentration was 0.53 mol/l in cyclohexane. The experiments were performed at 130 °C under argon flow. Symbols: valeraldehyde (white square), 2-pentylidenecyclopentanone **4** (black circle), 2-pentyl-2-cyclopent-1-one **5** (white circle), 2-propyl-3-hydroxyheptanal (+) **1**, 2-propylhept-2-enal (black up-pointing triangle) **2** and 1-hydroxy-2-pentylcyclopentanone (black square) **3**

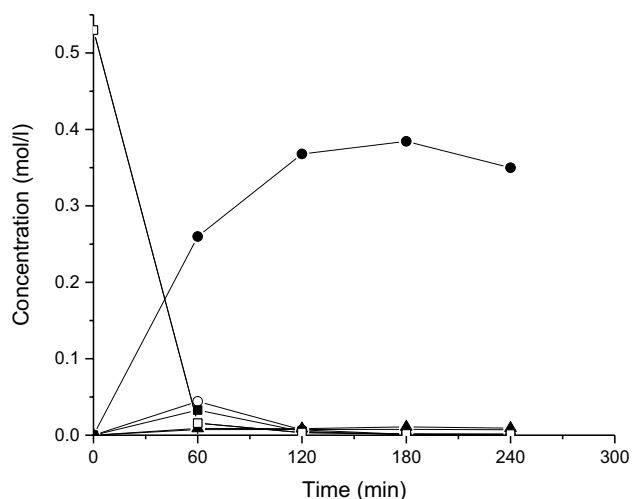


Fig. 10 Concentration of valeraldehyde and its self- and cross-condensation products as a function of time in valeraldehyde cross-condensation with cyclopentanone over FeO–MgO–DP. The initial valeraldehyde concentration was 0.53 mol/l in cyclohexane. The experiments were performed at 130 °C under argon flow. Symbols: valeraldehyde (white square), 2-pentylidenecyclopentanone **4** (black circle), 2-pentyl-2-cyclopent-1-one **5** (white circle), 2-propyl-3-hydroxyheptanal (+) **1**, 2-propylhept-2-enal (black up-pointing triangle) **2** and 1-hydroxy-2-pentylcyclopentanone (black square) **3**

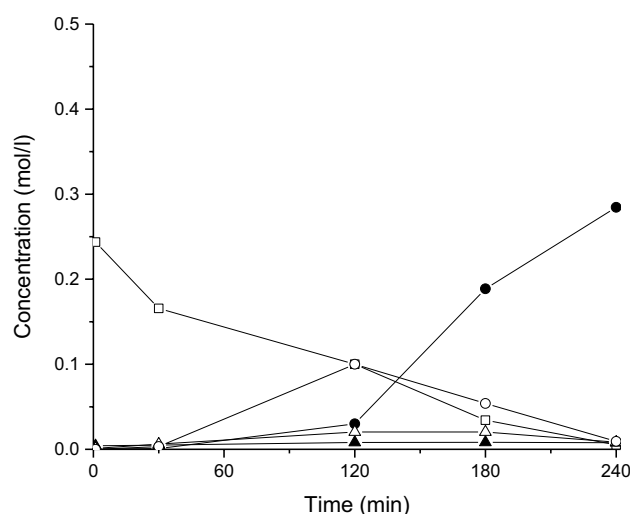


Fig. 12 Concentration of valeraldehyde and its self- and cross-condensation products as a function of time in valeraldehyde cross-condensation with cyclopentanone over CaO. The initial valeraldehyde concentration was 0.53 mol/l in cyclohexane. The experiments were performed at 130 °C under argon flow. Symbols: valeraldehyde (white square), 2-pentylidenecyclopentanone **4** (black circle), 2-pentyl-2-cyclopent-1-one **5** (white circle), 2-propyl-3-hydroxyheptanal (+) **1**, 2-propylhept-2-enal (black up-pointing triangle) **2** and 1-hydroxy-2-pentylcyclopentanone (black square) **3**

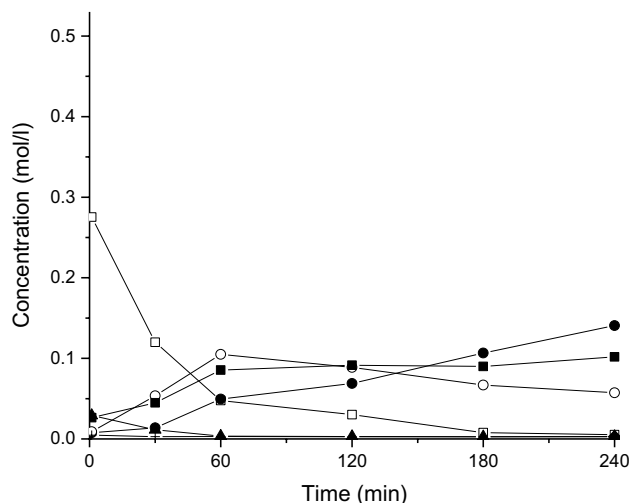


Fig. 11 Concentration of valeraldehyde and its self- and cross-condensation products as a function of time in valeraldehyde cross-condensation with cyclopentanone over CeO₂–MgO–DP. The initial valeraldehyde concentration was 0.53 mol/l in cyclohexane. The experiments were performed at 130 °C under argon flow. Symbols: valeraldehyde (white square), 2-pentylidenecyclopentanone **4** (black circle), 2-pentyl-2-cyclopent-1-one **5** (white circle), 2-propyl-3-hydroxyheptanal (+) **1**, 2-propylhept-2-enal (black up-pointing triangle) **2** and 1-hydroxy-2-pentylcyclopentanone (black square) **3**

to the presence of a conjugated double bonds, i.e. a carbonyl bond and a cyclic olefinic bond and high temperatures favor isomerization [2]. The sum of the reactant and product

concentrations was close to 100%. Since thermal aldol condensation of valeraldehyde–cyclopentanone showed promising results, it was worth to investigate the performance of catalysts at the same conditions. Valeraldehyde self-condensation is a thermodynamically feasible reaction even if approximate calculations of the Gibbs free energy for formation of the intermediate 2-propyl-3-hydroxyheptanal, gave a positive value.

Catalytic cross-condensation of valeraldehyde with cyclopentanone was investigated over two different FeO catalysts supported on MgO and CaO as well as CaO per se and CeO₂–MgO–DP (Table 6; Figs. 7, 8, 9, 10, 11, 12). The initial rates for valeraldehyde transformation decreased in the following order: FeO–MgO–DP > CeO₂–MgO–DP > FeO–CaO–EIM > CaO (Table 6). This order shows that the catalysts with the lowest basicity exhibited also the lowest initial valeraldehyde transformation rate, apart from a highly basic CaO. This could be explained by initial poisoning of CaO by traces of water and CO₂ despite drying over night at 100 °C in an oven. Based on the literature [39] dehydration of the basic catalysts is required to remove adsorbed water and CO₂. It is believed that this type of poisoning could easily occur for very basic CaO even in few minutes when loading the catalyst into the reactor. In addition when comparing the converted amounts of valeraldehyde after 120 min obtained with CaO (Fig. 12) and FeO–CaO–EIM (Fig. 11), it can be

seen that for neat CaO the conversion was only 83% compared with 99% obtained by FeO–CaO–EIM showing also that addition of just 10 wt% FeO increased activity of CaO.

Comparison of conversion levels over different catalysts shows that CaO, FeO–CaO–EIM and CeO₂–MgO–DP with strong basicity efficiently converted valeraldehyde. The conversion levels increased also with the increasing amount of strong basic sites (Fig. 8). The sums of the liquid phase products determined by GC (GCLPA) were high with FeO–MgO–DP and FeO–CaO–EIM, whereas CaO despite its high basicity exhibited a lower sum of reactant and product masses determined by GC analysis of the liquid phase.

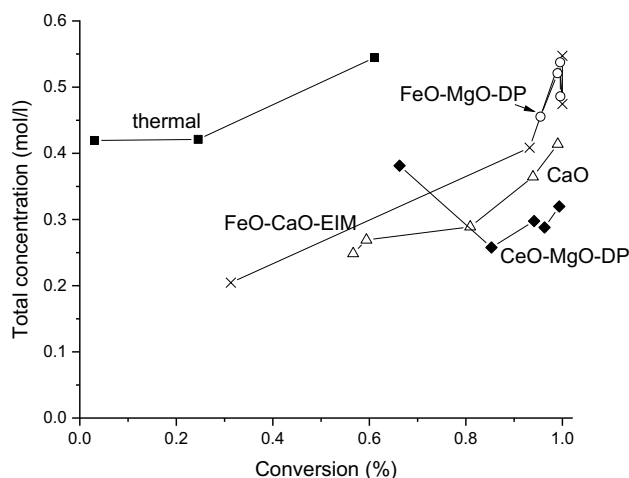


Fig. 13 A comparison of the total concentration, i.e. the sum of reactant and product concentrations from valeraldehyde self- and cross-condensation in the liquid phase, which are visible in GC analysis, as a function of conversion. The initial valeraldehyde concentration was 0.53 mol/l in cyclohexane. The experiments were performed at 130 °C under argon flow

These results may be related to formation of oligomers, in the latter case not visible in GC.

A comparison of the total concentration, i.e. the sum of the reactant and product concentrations from valeraldehyde self- and cross-condensation in the liquid phase, which are visible in GC analysis, as a function of conversion is shown in Fig. 13. The initial concentration of valeraldehyde was 0.53 mol/l and as it can be seen the highest total concentration is obtained in the absence of catalyst being after 3 h. In addition the total concentration increased with increasing conversion for those catalysts which were relatively good for catalyzing the formation of the desired product 4, i.e. FeO–CaO–EIM, FeO–MgO–DP and CaO. It can also be seen from Fig. 13 that the lowest total concentrations were obtained with CeO–MgO–DP and FeO–CaO–DP. The latter catalyst exhibited a very high concentration of acid sites most probably promoting oligomerisation.

Selectivity in the cross-condensation of valeraldehyde with cyclopentanone in comparison with valeraldehyde self-condensation can be evaluated by considering the ratio of the cross-condensation to valeraldehyde self-condensation products for thermal and catalytic experiments (Table 6) showing that this ratio was very low for the thermal reaction and reasonably high for catalytic experiments with basic catalysts. The yields of the desired product 4 and self-condensation product of valeraldehyde 2 over different catalysts after 4 h reaction illustrate that the highest yield of the desired product was obtained over FeO–MgO–DP followed by CaO and FeO–CaO–EIM (Table 6; Figs. 9, 10, 12). Repeatability in the cross condensation reactions was adequate showing for FeO–CaO–EIM catalyst minor deviations in the yield of the desired product 4, 42 ± 3%. All these catalysts exhibited strong basicity (Table 3). Intensive 2-propylhept-2-enal formation occurred only in the absence of heterogeneous catalysts. This result is in accordance with [1] where it was

Table 6 Results from valeraldehyde cyclopentanone cross condensation in thermal and catalytic experiments using cyclopentanone both as a solvent and reactant at 130 °C under argon flow

Entry	Catalyst	GCLPA (mol-%) after 4 h	Init. rate (mmol/min g _{cat})	Conversion (%) after 4 h	$\frac{\sum c_{0, VA}}{\sum c_{0, VA-CP}^b}$	Yield of 4 (mol-%)	Yield of 2 (mol-%)	Yield of 5 (mol-%)	Ratio between 4/2 after 4 h
1	Thermal	40 ^a	n.d	95 ^a	2.3	1	28	11	0.03
2	CeO ₂ –MgO–DP	60	0.17	99	0.54	26	<1	11	47
3	CaO	77	0.08	100	0.08	53	2	19	27
4	FeO–CaO–EIM	100	0.11	100	0.01	45	3	25	15
5	FeO–MgO–DP	92	0.27	95	0.07	66	2	19	33

2-pentylidenecyclopentanone 4, 2-propylhept-2-enal 2, isomer of 2-pentylidenecyclopentanone 5. GCLPA denotes the sum of the concentrations of valeraldehyde and its self- and cross condensation products visible in GC analysis. The initial valeraldehyde concentration was 0.53 mol/l, cyclopentanone was used both as a reactant and solvent

^a3 h

^b $\frac{\sum c_{0, VA}}{\sum c_{0, VA-CP}}$ denotes the initial ratio of the sum of the concentration VA self-condensation products/sum of the concentration of VA-CP cross condensation products

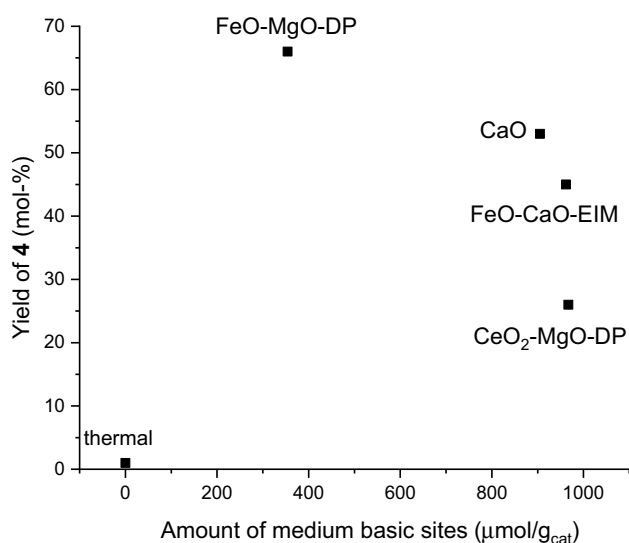


Fig. 14 The yield of 2-pentylidenecyclopentanone **4** h as a function of medium strong basic sites in the catalyst

concluded that formation of 2-propylhept-2-enal was the lowest with MgO and $\text{Al}_2\text{O}_3\text{-SiO}_2$, having acid-base site pairs.

The isomer of the desired product (e.g. compound **5**) was formed mainly over FeO-MgO-DP as well as over CaO and FeO-CaO-EIM showing that double bond migration occurs not only on acidic, but also on basic sites. According to ammonia TPD FeO-CaO-EIM, in which the iron containing phase is $\text{Ca}_2\text{Fe}_2\text{O}_5$, is also acidic promoting formation of the desired product isomer (Table 3; Fig. 9). When acidity of CeO₂-MgO-DP was lower, subsequently lower amounts of 2-hydroxy-2-pentylcyclopentanone were formed (Table 6, entry 2) compared to FeO-CaO-EIM (Table 6, entry 4).

Noteworthy is also that valeraldehyde self-condensation to form 2-propylhept-2-enal was concluded to be more acid catalyzed, when it was investigated [11] over a more acidic TiO₂ catalyst. In this work, however, self-condensation with a relatively highly acidic FeO-CaO-EIM was not able to produce high amounts of 2-propylhept-2-enal. In addition, activity of FeO-CaO-EIM catalyst was decreased after 60 min since dehydration of 2-hydroxy-2-pentylcyclopentanone to the desired product was inhibited (Fig. 9).

Only traces of 2,5-dipentylidene cyclopentanone **7** were formed despite its negative Gibbs free energy. This result indicates that consecutive condensation was retarded. Furthermore, all valeraldehyde has reacted after 120 min over FeO-MgO-DP, when the concentration of 2-pentylidenecyclopentanone was high indicating that valeraldehyde reacted already to some heavy compounds before that, since the GCLPA was 92%.

Esterification of valeraldehyde via the Tischenko reaction forming pentyl valerate **8** was not observed in this work in

line with the thermodynamic calculations, showing that such reaction is unfeasible in the studied temperature range.

Comparison of the yield of 2-pentylidenecyclopentanone **2** obtained by all catalysts at 4 h reaction time (Fig. 14) shows that an optimum amount of the largest total amount of basic sites is required for production of cross condensation products with the highest yield of **2** generated over FeO-MgO-DP. In [1] the conclusion was reached that either strongly acidic (e.g. $\text{Al}_2\text{O}_3\text{-SiO}_2$) or base catalysts, (e.g. MgO) are required, rather than bifunctional catalysts.

4 Conclusions

Ce-, Fe-modified CaO, CeO₂ and MgO base catalysts were successfully synthesized using deposition-precipitation (DP) and evaporation impregnation methods (EIM). The physico-chemical characterization of the catalysts using TPD-CO₂ showed the presence of the largest total amount of basic sites after CaO in FeO-CaO-EIM (1234 $\mu\text{mol/g}$) followed by CeO-MgO-DP (1087 $\mu\text{mol/g}$) catalyst. FeO-CaO-EIM catalyst resulted in the highest conversion (100%) of valeraldehyde during cyclopentanone cross-condensation with valeraldehyde. FeO-MgO-DP catalyst synthesized using the deposition precipitation method afforded the highest yield of the desired product 2-pentylidenecyclopentanone (66%), clearly indicating that the method of catalyst synthesis has a tremendous influence on conversion and selectivity to the desired products. Correlation of valeraldehyde conversion with the amount of medium strong basic sites revealed that these sites affect the aldol condensation reaction.

Acknowledgments Open access funding provided by Abo Akademi University (ABO).

Open Access This article is distributed under the terms of the Creative Commons Attribution 4.0 International License (<http://creativecommons.org/licenses/by/4.0/>), which permits unrestricted use, distribution, and reproduction in any medium, provided you give appropriate credit to the original author(s) and the source, provide a link to the Creative Commons license, and indicate if changes were made.

References

1. Hasni M, Prado G, Rouchaud J, Grange P, Devillers M, Delsarte S (2006) *J Mol Catal A Chem* 247:116–123
2. Xu J, Cao Y, Ma Q, Peng X (2013) *Asian J Chem* 25:3847–3849
3. Xie J, Zhang L, Zhang X, Han P, Xie J, Pan L, Zou DR, Liu SH, Zou JJ (2018) *Sust Energy Fuels* 2:1863–1869
4. Deng Q, Xu J, Han P, Pan L, Wang L, Zhang X, Zou JJ (2016) *Fuel Proc Tech* 148:361–366
5. Kwong TL, Yung KF (2015) *RSC Adv* 5:83748–83756
6. Mahrwald R, Schick H (1990) *Synthesis* 7:592–595
7. Han Z, Yorimitsu H, Hideki S, Hiroshi S, Oshima K (2000) *Tetrahedron Lett* 41(22):4415–4418C

8. Martin A (1998) US patent 5776884
9. Fujisawa H, Kondou Y, US patent (2005) 2005/0009928 A1
10. Liang D, Li G, Liu Y, Wu J, Zhang X (2016) *Catal Comm* 81:33–36
11. Deng Q, Nie G, Pan L, Zou J-J, Zhang X, Wang L (2015) *Green Chem* 17:4473–4481
12. Poncet AF (1982) FR patent, 2500477
13. Zhao L, An H, Zhao X, Wang Y (2016) *Ind Eng Chem Res* 55:12326–12333
14. Tang Z, Zhou Y, Feng Y (2004) *Appl Catal A Gen* 273:171–176
15. Vrbkova E, Tisler Z, Vyskocilova E, Kadlec D, Cerveny L (2018) *Chem Technol Biotech* 93:166–173
16. Vit Z, Nondek L, Malik J (1982) *Collect Czech Chem Commun* 47:2235–2245
17. Vrbkova E, Vyskocilova E, Krupka J, Cerveny L (2016) *Progr React Kinet Mech* 41:289–300
18. MAUD. <http://www.ing.unitn.it/~maud/>. Accessed 8 Dec 2018
19. Powder Diffraction File 2 (PDF-2), sets 1–46, 1996 release, International Centre for Diffraction Data (ICDD)
20. Inorganic Crystal Structure Database (ICSD) <http://www.fiz-karlsruhe.de/icsd.html>. Accessed 8 Dec 2018
21. Crystallography Open Database <http://www.crystallography.net/cod/index.php>. Accessed 8 Dec 2018
22. Chesnokov B, Bazhenova L (1985) *Zap Vses Mineral O-va* 114:195–196.20. Germany, ICDD Grant-in-Aid
23. Yang S, Zhang X, Chen L, Sun L, Xie X, Zhao B (2017) *J Anal Appl Phys* 125:1–8
24. Morris MC, McMurdie HF, Evans EH, Paretzkin B, Parker HS, Pyrros NP (1983) *Standard X-ray Diffraction Powder Patterns*, NBS Monograph 25 - Section 20, National Bureau of Standards, p 38
25. Swanson HE, Tatge E (1953) *Natl Bur Stand (US) Circ* 539(I):15
26. Swanson HE, Tatge E (1953) *Natl Bur Stand (US) Circ* 539(I):15.24
27. Morris MC, McMurdie HF, Evans EH, Paretzkin B, Parker HS, Panagiotopoulos NC (1981) *Standard X-ray Diffraction Powder Patterns*, NBS Monograph 25 - Section 18, National Bureau of Standards, p 37
28. Kern A, Doetzer R, Eysel W (1993) *Mineralogisch-Petrographisches Inst., Univ. Heidelberg. Germany, ICDD Grant-in-Aid*, (1993)
29. Yang J, Li N, Li S, Wang W, Wang A, Wang X, Cong Y, Zhang T (2014) *Green Chem* 16:4879–4884
30. Ye L, Lin H, Zhou H, Yuan Y (2010) *J Phys Chem C* 114:19753–19760
31. Ferretto L, Glisenti A (2002) *J Mol Catal A: Chem* 187:119–128
32. Miles WH, Nutaitis CF, Anderton CA (1996) *Chem Educ* 73:272
33. Dumitriu E, Hulea V, Fecete I, Auroux A, Lacaze JF, Guimon C (2001) *Micropor Mesop Mater* 43:341–359
34. Nemansky MW, Abbott MM, Van Ness HC (1975) *Basic engineering thermodynamics*. McGraw-Hill, New York
35. Poling BE, Prausnitz JM, O'Connell JP (2004) *The properties of gases and liquids*, 5th edn. McGraw-Hill, New York
36. Joback KG (1984) A unified approach to physical property estimation using multivariate statistical techniques, Thesis SM, Department of Chemical Engineering, Massachusetts Institute of Technology, Cambridge, MA
37. Joback KG, Reid RC (1987) *Chem Eng Comm* 57:233–243
38. Heinz AS, Gonzales JE, Fink MJ, Mitchell BS (2008) *J Mol Catal A Chem* 304:117–120
39. Hattori H (1995) *Chem Rev* 95:537–558

Publisher's Note Springer Nature remains neutral with regard to jurisdictional claims in published maps and institutional affiliations.